

# ULTRASOUND ASSISTED SINGLE SCREW EXTRUSION PROCESS FOR DISPERSION OF CARBON NANOFIBERS IN POLYMERS

Avraam I. Isayev, Changdo Jung and Kaan Gunes  
*Institute of Polymer Engineering*  
*The University of Akron*  
*Akron, Ohio 44325-0301*

## Abstract

A novel method for the continuous dispersion of carbon nanofibers (CNFs) in a polymer matrix for manufacturing high performance nanocomposites was developed using an ultrasonically assisted single screw extrusion process. The effect of ultrasound on die pressure, electrical conductivity, rheological, morphological and mechanical properties of polyetherimide (PEI) filled with 1-20 wt% CNFs was studied. A reduction in the die pressure, percolation threshold and an increase in the viscosity, Young's modulus and electrical conductivity along with better CNF dispersion in nanocomposites was achieved through ultrasonic treatment.

## Introduction

Polymer nanocomposites containing CNFs often exhibit properties superior to conventional fiber-reinforced composites [1]. Among them, CNF/polyimide nanocomposites were studied [2]. The CNF's are produced by the catalytic decomposition of hydrocarbons in the vapor phase at 500-1500°C [3]. CNFs are readily aggregate and bundle together or become entangled. Dispersion of the individual fibers is the main obstacle for their use in many applications [4]. The commonly used methods to disperse CNFs are mechanical, melt processing and plasma treatment. Among these methods ultrasonication of CNFs in solutions for a prolonged time (minutes and hours) is used [5]. This is a batch process and the prolonged ultrasonication introduces defects resulting in shorter CNFs which may adversely affect many of their attractive properties [6]. Melt processing of the high viscosity of polymer/CNF mixtures is utilized through high shear mixing in the extruder [7-13] and internal mixer [7, 14-17]. These methods have environmental advantages as they are solvent free processes. Plasma coating is used to enhance the dispersion of the CNFs in the polymer matrix [18]. In-situ polymerization is also utilized to keep bundles of CNFs dispersed in the polymer matrix [19]. As reviewed in [20], some other methods have been attempted for enhancing dispersion, like in-situ production of CNFs, but found limited success.

Recently, the use of high power ultrasound in extrusion process was proposed for dispersion of nanosize

silica fillers [21] and intercalation and exfoliation of nanoclays [22-24] in polymers with a residence time of ultrasonic treatment of only a few seconds.

The present study describes preparation of CNF/PEI nanocomposites obtained by means of extrusion in a novel ultrasonic compounding extruder. Mechanical, rheological, electrical, and thermal properties of the obtained nanocomposites were studied. Effects of the processing parameters on dispersion of CNFs in PEI were also elucidated.

## Experimental

### Materials

CNFs, Pyrograf-III, PR-19-HT, were provided by Applied Sciences, Inc., Cedarville, OH, and used without any further purification. PEI, Ultem 1000P, in powder form from GE Plastics was used as received. Mixtures of various concentrations of the PEI powder and CNFs were prepared by dry mixing using ball milling for 24 hrs. The mixtures were then dried under vacuum at 120°C for a minimum of 24 hrs prior to processing.

### Equipment and Procedures

A single screw ultrasonic compounding extruder having a screw diameter of 25.4 mm and a L/D ratio of 33:1 was used. It was built based on a Killion extruder with L/D of 24. The ultrasonic extruder was equipped with a UCM and two Melt Star mixers along with the ultrasonic treatment zone along the barrel. A schematic drawing of the ultrasound extruder is shown in Figure 1. Two 6 kW ultrasonic units consisting of power supplies, converters, boosters and horns were used to generate ultrasonic waves at a frequency of 20 KHz. Cylindrical horns of 25.4 mm diameter were used. The gap opening for the flow of compound in ultrasonic zone was kept at 2.54 mm. The mean residence time in the ultrasonic treatment zone was 7 s at a flow rate of 15 g/min. The extrusion temperature was varied from 320 to 340°C from the feed zone to the die. Screw speeds of 30, 60 and 100 rpm for flow rate of 15 g/min were used. The ultrasonic treatment was carried out at various amplitudes. Unfilled PEI was also processed using the same procedure to produce a control sample.

Microscopic analysis of injection and compression moldings was conducted by means of SEM. ARES was used to measure the storage ( $G'$ ) and loss ( $G''$ ) moduli at a

fixed strain amplitude of 2% in dynamic frequency sweep mode at 340°C. Instron tensile testing machine was used to carry out tensile tests at a crosshead speed of 5 mm/min at room temperature on specimens prepared by a HAAKE mini-jet molder at a melt and mold temperature of 340°C and 120°C, respectively.

Disks with a thickness of 1 mm and a diameter of 60 mm were prepared by compression molding to measure the electrical volume resistivity by means of an electrometer, Kiethley Instrument Model No.6517A, attached to an 8009 test fixture was used. A voltage of 10V was applied for 60 s in the test.

## Results and Discussion

### Process Characteristics

The entrance pressure and temperature of the ultrasonic treatment zone as a function of ultrasonic amplitude is presented in Figure 2. The entrance pressure is substantially reduced as the ultrasonic amplitude is increased. This decrease of pressure is caused by the combined effect of the reduced viscosity of materials and reduction in friction of polymer melt along the die wall [25]. It is also evident from Figure 2 that the pressure increases with increasing CNF concentration. It is interesting to note that the pressure increases slightly up to 15 wt% and increased significantly at 20 wt% CNF concentration. Such a behavior is apparently attributed to the percolation threshold at 20 wt% CNF/PEI composites. It is also noted from Figure 2 that the temperature at the ultrasonic treatment zone increases with increasing ultrasonic amplitude.

The ultrasonic power consumption during ultrasonic treatment of PEI at various CNF concentrations as a function of ultrasonic amplitude is shown in Figure 3. This set of data is obtained at 60 rpm. Upon increase of the CNF content from 0 to 20 wt%, an increase of the power consumption was observed with an increase of amplitude. Similar to the observation made on nanoclay dispersion in polymers [22], a higher energy is also required to disperse CNFs.

### Rheology

Figure 4 shows the complex viscosity as a function of frequency for the untreated and ultrasonically treated CNF/PEI nanocomposites containing 0 to 20 wt% CNFs. The viscosities of CNF/PEI composites increase with increasing CNF content. Viscosity of ultrasonically treated composites is consistently higher compared to that of untreated ones. At the same time, viscosity of virgin PEI slightly decreases with ultrasonic treatment. The viscosity of nanocomposites obtained at an amplitude of 10  $\mu\text{m}$  shows slightly lower values than those at amplitudes of 5  $\mu\text{m}$  and 7.5  $\mu\text{m}$ . This is not only because of the thermomechanical degradation of polymer, but also because of a possible breakage of nanofibers during ultrasonic treatment. This explanation is supported by

experimental results of the length of CNFs extracted from composites as shown below. As the CNF concentration is increased, viscosity of the nanocomposites exhibits stronger frequency dependence at low frequencies. Such a frequency dependence and, therefore, stronger shear thinning is especially pronounced for ultrasonically treated composites. This strong shear thinning behavior can be attributed to a greater degree of polymer-CNF interaction due to dispersion of the CNFs leading to a reduction of the percolation threshold in nanocomposites. It means that the viscosity curve is a possible tool for identifying the presence of the percolation threshold for these composites [17]. At low frequencies, the viscosity seems to exhibit a percolation threshold at around 15 wt% of CNF's, as seen in Figure 5. This confirms that the nanocomposite at concentrations between 15% and 20% CNFs passes through the percolation threshold evidently created by a better dispersion of CNFs by ultrasonic treatment. This effect is not seen on untreated nanocomposites.

### Electrical Conductivity

Figure 6 shows the electrical volume resistivity of nanocomposites as a function of CNF concentration. For ultrasonically treated composites, the resistivity at 15 wt% of CNF loading dropped by about 2 orders of magnitude. At the same time, a similar drop in the resistivity of nanocomposites extruded without ultrasonic treatment occurs at 17 wt% CNF loading. These concentrations correspond respectively to the onsets of percolation. The volume resistivity is dependent not only on the fiber concentration, but also on the fiber length and their

dispersion. Clearly, ultrasonic treatment leads to an improved dispersion of the CNFs. It is also seen from Figure 6 that composites prepared by ball milling show percolation threshold at much lower CNF concentration (4 wt %). This is due the presence of long and aggregated fibers in these composites.

### Microscopic Analysis

Figure 7 shows SEM micrographs of CNFs as received. They have large aspect ratios (> 100). The diameters of these nanofibers vary from 70 nm to 200 nm

and sizes of their bundles range from 10  $\mu\text{m}$  to 50  $\mu\text{m}$ . After ball milling of CNFs with PEI powder, the bundles of CNFs remain. Interwoven bundles and aggregates of CNFs up to 50  $\mu\text{m}$  in size were observed in SEM micrographs as shown in Figure 8. Figure 9 depicts SEM micrographs of fractured surfaces of 15 wt% CNF/PEI nanocomposites without and with ultrasonic treatment at an amplitude of 10  $\mu\text{m}$ . The CNFs are clustered in the matrix with about 2~5  $\mu\text{m}$  diameter in untreated composites. In the treated nanocomposites CNFs are not clustered but still in contact with each other. The latter could be the reason why the percolation threshold is

achieved at a lower concentration of about 15 wt% in ultrasonically treated nanocomposites.

Figure 10 shows the SEM micrograph of CNFs extracted from the nanocomposite. As seen from this figure, the length of extracted CNFs is 2~10  $\mu\text{m}$  which is lower than their initial length of 30~100  $\mu\text{m}$  reported by Applied Sciences, Inc. The degradation of fiber length is not only attributed to the high shear in extruder [19] but also to the action of ultrasound. In particular, Figure 11 shows the length distribution of CNFs in nanocomposites obtained without and with ultrasonic treatment, respectively, at a screw rotation speed of 60 rpm. Only a slight decrease in the fiber length due to ultrasonic treatment is observed.

### Mechanical Properties

Ultrasonic treatment at an amplitude of 5 and 7.5  $\mu\text{m}$  leads to an increase in the Young's modulus of the nanocomposites (Figure 12). Values of the modulus of samples after ball milling are lower than those of extruded composites. The strength of PEI/CNF nanocomposites showed little change with ultrasonic treatment. (Figure 13). Also, the strength of nanocomposites does not change up to 15% loading and then slightly decreases. This behavior is attributed to the lack of adhesion between CNFs and PEI matrix. The explanation is supported by the detachment of fibers seen in SEM micrographs depicted in Figure 9. The strength of composites obtained after ball milling is considerably lower in comparison with those of extruded composites.

### Conclusions

CNF/PEI nanocomposites with CNF contents up to 20 wt% have been prepared by means of a novel ultrasonic single screw compounding extruder. Based on rheological and electrical conductivity measurements, the estimated percolation threshold in ultrasonically treated CNF/PEI nanocomposites is found to be lower than those of untreated nanocomposites. Furthermore, it was established that high power ultrasound is effective in obtaining relatively homogeneous dispersion with improved electrical and thermal conductivity in the CNF/PEI nanocomposites. An increase of the Young's modulus in CNF/PEI nanocomposites was recorded under ultrasonic treatment, without reduction in the tensile strength. SEM micrographs of dry-mixed PEI/CNF composites by ball milling indicated the presence of CNF bundles. The CNF bundles are absent after compounding using an ultrasonic single screw extruder with ultrasonic treatment.

### Acknowledgement

Authors wish to thank the NASA Headquarters for their financial support of this study.

### References

1. Ajayan, P. M., Schadler, L. S., and Braun, P. V., *Nanocomposite Science and Technology*, Weinheim, Wiley, 2003
2. Hergenrother, P. M., *High Performance Polym.*, 2003; 15: 3-45.
3. Mordkovich, V. Z., *Theoretical Foundations of Chemical Engineering*, 2003; 37: 429-438.
4. Johnson, J. A., Barbato, M. J., Hopkins, S. R., and O'malley, M. J., *Prog Org Coat*, 2003; 47: 198-206.
5. Zhao, J., Schaefer, D. W., Shi, D., Lian, J., Brown, J., Beaucage, G., Wang, L., and Ewing, R. C., *J Phys Chem B*, 2005; 109: 23351-23357.
6. Gauthier, C., Chazeau, L., Prasse, T., and Cavaille, J. Y., *Compos Sci Technol*, 2005; 65: 335-343.
7. Ma, H., Zeng, J., Realff, M. L., Kumar, S., and Schiraldi, D. A., *Compos Sci Technol*, 2003; 63: 1617-1628.
8. Carneiro, O. S., Covas, J. A., Bernardo, C. A., Caldeira, G., Van Hattum, F. W. J., Ting, J. M., Alig, R. L., and Lake, M. L., *Compos Sci Technol*, 1998; 58: 401-407.
9. Hammel, E., Tang, X., Trampert, M., Schmitt, T., Mauthner, K., Eder, A., and Potschke, P., *Carbon*, 2004; 42: 1153-1158.
10. Kuriger, R. J. and Alam, M. K., *Polym Compos*, 2001; 22: 604-612.
11. Kuriger, R. J., Alam, M. K., Anderson, D. P., and Jacobsen, R. L., *Compos, Part A: Appl Sci Manuf* 2001; 33A: 53-62.
12. Hine, P., Broome, V., and Ward, I., *Polymer*, 2005; 46: 10936-10944.
13. Zeng, J., Saltysiak, B., Johnson, W. S., Schiraldi, D. A., and Kumar, S., *Compos, Part B: Eng*, 2004; 35B: 245-249.
14. Lozano, K. and Barrera, E. V., *J Appl Polym Sci*, 2000; 79: 125-133.
15. Yang, S., Lozano, K., Lomeli, A., Foltz, H. D., and Jones, R., *Compos, Part A: Appl Sci Manuf*, 2005; 36A: 691-697.
16. Lozano, K., Yang, S., and Zeng, Q., *J Appl Polym Sci*, 2004; 93: 155-162.
17. Lozano, K., Bonilla-Rios, J., and Barrera, E. V., *J Appl Polym Sci*, 2001; 80: 1162-1172.
18. Shi, D., Lian, J., He, P., Wang, L. M., Xiao, F., Yang, L., Schulz, M. J., and Mast, D. B., *Appl Phys Lett*, 2003; 83: 5301-5303.
19. Higgins, B. A. and Brittain, W. J., *Europ Polym JI*, 2005; 41: 889-893.
20. Breuer, O. and Sundararaj, U., *Polym Compos*, 2004; 25: 630-645.
21. Isayev, A. I., Hong, C. K., and Kim, K. J., *Rubber Chem Technol*, 2003; 76: 923-947.
22. Lapshin, S. and Isayev, A. I., SPE ANTEC, 2005; 63rd: 1911-1915.
23. Lapshin, S. and Isayev, A. I., SPE ANTEC, 2006; 64<sup>th</sup>: 602-606.
24. Swain, S. K. and Isayev, A. I., SPE ANTEC, 2006; 64<sup>th</sup>: 923-927.

**Keywords:**

Ultrasound, Carbon nanofibers, PEI, Dispersion.

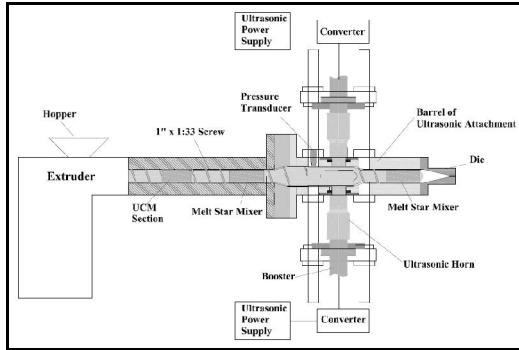


Figure 1. The ultrasonic extruder

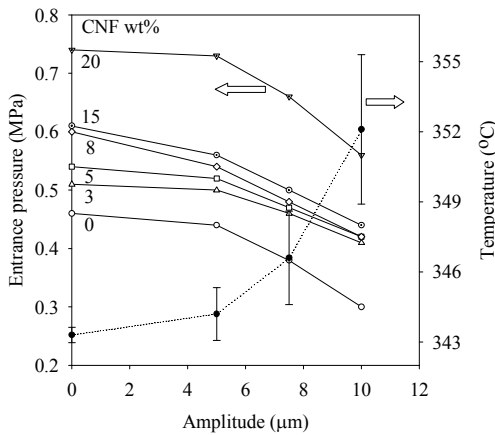


Figure 2. Entrance pressure in front of ultrasonic treatment zone and melt temperature in the ultrasonic treatment zone as a function of amplitude at various CNF concentrations at 60 rpm.

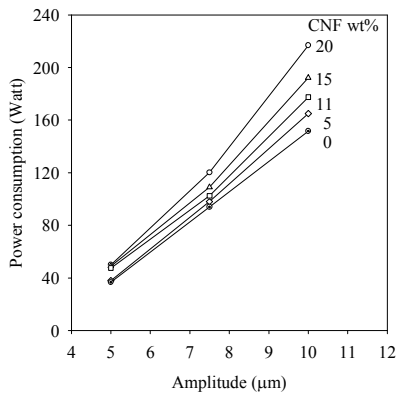


Figure 3. Ultrasonic power consumption as function of ultrasonic amplitude for PEI nanocomposites at various CNF concentrations at 60 rpm.

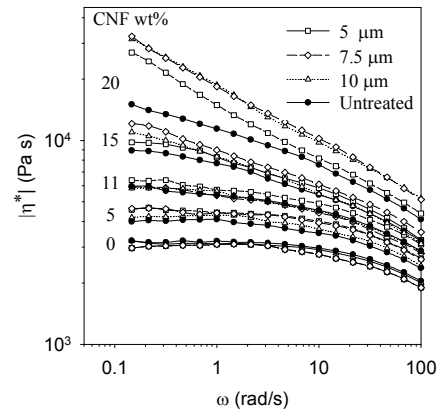


Figure 4. Complex viscosity as a function of frequency for untreated and ultrasonically treated CNF/PEI nanocomposites containing 0 to 20 wt% CNFs obtained at various ultrasonic amplitudes at 60 rpm.

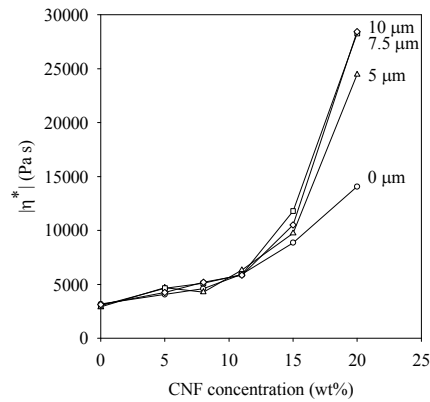


Figure 5. Complex viscosity at a frequency of 0.2 s<sup>-1</sup> as a function of CNF concentration for untreated and ultrasonically treated composites obtained at various ultrasonic amplitudes at 60 rpm.

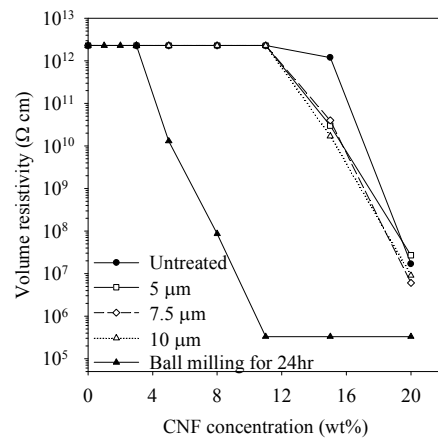


Figure 6. Volume resistivity of nanocomposites as a function of CNF concentration obtained at various ultrasonic amplitudes at 60 rpm and after ball milling.

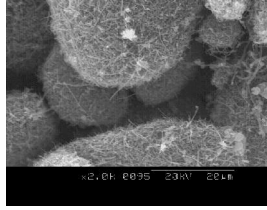


Figure 7. SEM micrograph of CNFs as received.

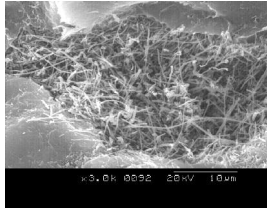


Figure 8. SEM micrographs of cryofractured surface of nanocomposite containing 3 wt% CNFs prepared by ball milling and injection molding.

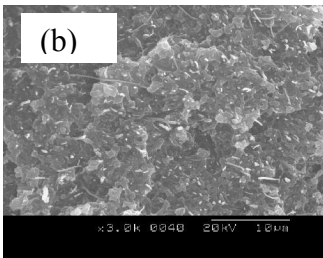
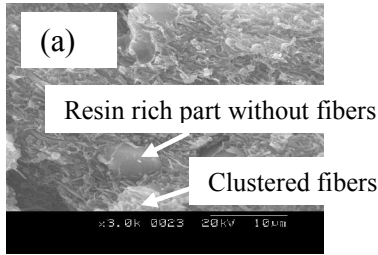


Figure 9. SEM micrographs of cryofractured surface of injection molding of 15 wt% CNF/PEI nanocomposites obtained without (a) and with (b) ultrasonic treatment at an amplitude of 10  $\mu\text{m}$  at 60 rpm.

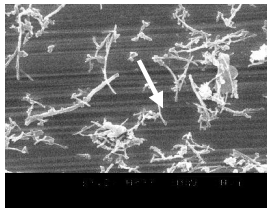


Figure 10. SEM micrographs of CNFs extracted from untreated 11 wt% CNF/PEI nanocomposites at 60 rpm.

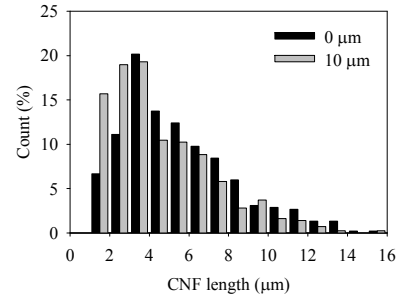


Figure 11. Effect of ultrasound on length distribution of CNFs for 15 wt% CNF/PEI nanocomposites at 60 rpm.

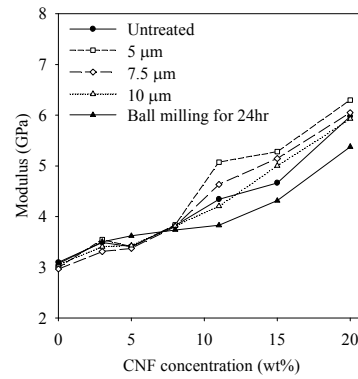


Figure 12. Young's modulus of CNF/PEI nanocomposites as a function of CNF concentration without and with ultrasonic treatment at various ultrasonic amplitudes at 60 rpm and after ball milling.

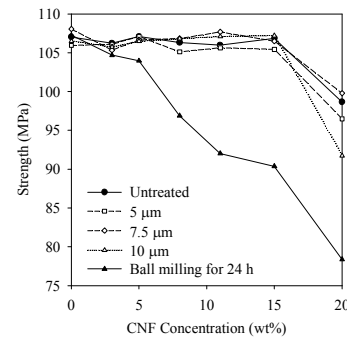


Figure 13. Strength vs. CNF concentration of CNF/PEI nanocomposites obtained without and with ultrasonic treatment at different amplitudes at 60 rpm and after ball milling.